Integrity Monitoring Techniques in GPS/Galileo

João Pedro Duque Duarte
joao.d.duarte@ist.utl.pt

Instituto Superior Técnico, Lisboa, Portugal

May 2015

Abstract

The use of navigation systems in aviation requires a high level of trust in the solution to be used. Integrity is defined as the measure of the trust that can be placed in the correctness of the information supplied by a navigation system. There are several architectures that allow to compute the integrity levels on a solution provided by the system. One of those architectures are the integrity monitoring techniques called RAIM and these consist in algorithms implemented at the receiver and allow to measure the integrity level and in case of a faulty satellite that fault is not only detected but the faulty satellite may be excluded. There are several integrity algorithms, namely the Least-Squares-Residuals and the Range-Comparison-Method that were analysed in this thesis. Integrity monitoring algorithms have their performance affected by satellites geometry. Thus, it is important to compare both the considered algorithms as its performance in different geometry cases. The results show that both algorithms have similar performances whereby the major difference is at the complexity level, which is considerable higher in the Range-Comparison-Method case.
Keywords: GPS, Galileo, Integrity, RAIM

1. Introduction

Nowadays various Global Navigation Satellite Systems (GNSS) are used worldwide providing the user with its position. Examples of GNSS systems are the Global Positioning System (GPS) from United States and Galileo from Europe. These systems consist in a space segment composed by a satellite constellation, a ground segment constituted by a network of ground stations that perform the necessary tasks to maintain the proper operation of the system and a user segment that is composed by users equipped with a receiver capable of using signals from the space segment. The applications of such systems have been increasing in the past years. As there is a wide range of applications not all have the same requirements. Some just need a rough estimate of the user position while others require significantly more accuracy and integrity.

2. Fundamentals

2.1. Measurement Errors

There are a number of error sources that can corrupt the measurements from each satellite. The errors are often categorized as *noise* or *bias*. Noise generally refers to a quickly varying error that averages to zero over a short period of time. A bias tends to persist over a period of time.

These sources can be grouped according to their origin, and can be categorized in three groups [14]:

- Errors in the parameters values broadcast by a satellite in its navigation message;
- Uncertainties associated with propagation medium which affect the travel time of the signal from a satellite to the receiver (includes ionospheric and tropospheric effects);
- Receiver noise which affects the precision of a measurement, and interference from signals reflected from surfaces in the proximity of the antenna (includes thermal noise and multipath effects).

2.1.1 Pseudorange Error Budget

The combination of these errors is known as User Equivalent Range Error (UERE) and corresponds to the root-sum-squared of the components that contribute to measurements errors. These errors are considered independent Gaussian random variables [5], thus the UERE can be identically distributed by the satellites. The value of the system UERE error is 7.1 meters (1σ).

3. Position determination

Let's consider

$$D_i = \sqrt{(X_i - x_R)^2 + (Y_i - y_R)^2 + (Z_i - z_R)^2} \quad (1)$$

the distance between the satellite i with coordinates (X_i, Y_i, Z_i), and the receiver with coordinates

(x_R, y_R, z_R).

GPS receivers receive and decode signals from satellites with information about their positions, enabling the receivers to compute their own position [10].

Let's consider $\tilde{t}_R$ is the nominal time (time indicated by the clock) on the receiver at the time of signal reception and $\tilde{t}_i$ the nominal time on the satellite at time of signal output. The time on the satellites is obtained by the set of atomic clocks while the time on the receiver is obtained by a quartz clock with a much lower accuracy. The relations between nominal time and real time t_i and t_R are $\tilde{t}_R = t_R + \Delta t_R$ and $\tilde{t}_i = t_i + \Delta t_i$ where Δt_i and Δt_R are respectively the clock errors of the satellite and receiver. Generally $|\Delta t_i| \ll |\Delta t_R|$.

Pseudorange is a distance measured between the satellite and the receiver

$$\rho_i = (\tilde{t}_R - \tilde{t}_i)c \tag{2}$$

where c is the light speed.

The pseudorange ρ_i would be equal to the geometric distance R_i if the propagation medium was vacuum and if there were no clock errors or other disturbances to the signal propagation. As this is not the case these distances are not coincident.

To determine the user position (x_u, y_u, z_u) and clock offset t_u, pseudorange measurements are made relatively to M satellites, with $M \geq 4$, resulting in [10]:

$$\rho_i = \sqrt{(X_i - x_u)^2 + (Y_i - y_u)^2 + (Z_i - z_u)^2} + ct_u + \epsilon_i \tag{3}$$

where

ρ_i	:	pseudorange
(X_i, Y_i, Z_i)	:	coordinates of satellite i
(x_u, y_u, z_y)	:	coordinates of the user
ϵ_i	:	measurement error associated with ρ_i

Generally these errors are considered independent, Gaussian, zero mean and equal variance.

As the equations are nonlinear there are several methods that can be used to obtain a solution, namely [5]:

1. Bancroft algorithm;
2. Iterative solutions;
3. Kalman filtering.

3.1. Position solution using Kalman Filter

Extended Kalman Filter is frequently used as an alternative to Least Squares to obtain a solution for the navigation equation. The observables are incorporated in discrete time intervals, in this case of 1 second, and the observation model is linearised relatively to the best state estimate. The x_k state has five, eight or eleven components (depending on the model chosen) including two components for the receiver clock model [16].

The number of space components depends on the dynamics model chosen. This model is usually chosen according to the type of trajectory expected. The model used in this thesis was the *PV model*. When we have a receiver in motion it is convenient to use a *PV model* (position + velocity) with a state vector dimension of 8 (3 position coordinates + 3 velocity coordinates + 2 clock components).

In the *PV* model each coordinate is modelled as an integrated Brownian motion.

A simple clock model is defined as a state vector with dimension two, in which frequency and phase show variations of Brownian motion in reasonable time intervals.

3.1.1 Extended Kalman filter: dynamics models

The dimensions of the dynamics models depend on the model used.

PV model The state space equation of the discrete time model for the x_u coordinate is:

$$\begin{bmatrix} x_{1,k+1} \\ x_{2,k+1} \end{bmatrix} = \begin{bmatrix} 1 & \Delta t \\ 0 & 1 \end{bmatrix} \begin{bmatrix} x_{1,k} \\ x_{2,k} \end{bmatrix} + \begin{bmatrix} u_{1,k} \\ u_{2,k} \end{bmatrix} \tag{4}$$

where the covariance noise matrix is

$$Q_k = E[u_{1,k}u_{2,k}]^T[u_{1,k}u_{2,k}] = q_v \Delta t \begin{bmatrix} \frac{(\Delta t)^2}{3} & \frac{\Delta t}{2} \\ \frac{\Delta t}{2} & 1 \end{bmatrix} \tag{5}$$

and q_v is a selectable parameter.

If $x_k = [x_{1,k} \dots x_{8,k}]^T$ is the state vector in which $x_{1,k}$ and $x_{2,k}$ are the position and velocity of the x_u user coordinate, $x_{3,k}$ and $x_{4,k}$ are the position and velocity of the y_u user coordinate and $x_{5,k}$ and $x_{6,k}$ are the position and velocity of the z_u user coordinate, the dynamics model in discrete time is given by

$$\begin{bmatrix} x_{1,k+1} \\ x_{2,k+1} \\ x_{3,k+1} \\ x_{4,k+1} \\ x_{5,k+1} \\ x_{6,k+1} \\ x_{7,k+1} \\ x_{8,k+1} \end{bmatrix} = \underbrace{\begin{bmatrix} 1 & \Delta t & & & & & & \\ & 1 & & & & & 0 & \\ & & 1 & \Delta t & & & & \\ & & & 1 & & & & \\ & & & & 1 & \Delta t & & \\ & & & & & 1 & & \\ & 0 & & & & & 1 & \Delta t \\ & & & & & & & 1 \end{bmatrix}}_{\Phi_k} \begin{bmatrix} x_{1,k} \\ x_{2,k} \\ x_{3,k} \\ x_{4,k} \\ x_{5,k} \\ x_{6,k} \\ x_{7,k} \\ x_{8,k} \end{bmatrix} + \begin{bmatrix} u_{1,k} \\ u_{2,k} \\ u_{3,k} \\ u_{4,k} \\ u_{5,k} \\ u_{6,k} \\ u_{7,k} \\ u_{8,k} \end{bmatrix} \tag{6}$$

where Φ_k is the dynamics matrix.

3.1.2 Extended Kalman filter: observations model

The dynamics equations are linear for the dynamics model implemented, but the observation's equation

$$z_k = h[x(t_k)] + v_k \tag{7}$$

is nonlinear. In (7) $z_k = [\rho_{1,k} \dots \rho_{n,k}]^T$, with $n \geq 4$, is the measured pseudoranges vector and

$$h[x] = \begin{bmatrix} \sqrt{(\widetilde{x}_1 - x_a)^2 + (\widetilde{y}_1 - x_b)^2 + (\widetilde{z}_1 - x_c)^2} + x_d \\ \vdots \\ \sqrt{(\widetilde{x}_n - x_a)^2 + (\widetilde{y}_n - x_b)^2 + (\widetilde{z}_n - x_c)^2} + x_d \end{bmatrix} \tag{8}$$

where $\widetilde{x}_i$, $\widetilde{y}_i$ and $\widetilde{z}_i$ are the satellite coordinates of the i satellite, with $i = 1, \dots, n$ and x_a, x_b, x_c and x_d are the state vector components of x_u, y_u, z_u and $x_\phi c$. The covariance noise matrix of the observations is

$$R_k = \begin{bmatrix} \sigma^2_{1,UERE} & & 0 & \\ & \sigma^2_{2,UERE} & & \\ & & \vdots & \\ & 0 & & \sigma^2_{n,UERE} \end{bmatrix} \tag{9}$$

If all the variances of the several pseudoranges are equal to σ^2_{UERE}, R_k will be given by

$$R_k = \sigma^2_{UERE} \times I \tag{10}$$

The observation's matrix of the generalised Kalman filter is

$$H_k = \left[\frac{\partial h_i[\hat{x}(k \mid k-1)]}{\partial x_j} \right]_{(n \times l)} \tag{11}$$

where n is the satellite number and l is the state vector dimension, depending on the dynamics model adopted. For the PV model $l = 8$

$$H_k = - \begin{bmatrix} a_{x1} & 0 & a_{y1} & 0 & a_{z1} & 0 & -1 & 0 \\ \vdots & \vdots & \vdots & \vdots & \vdots & \vdots & \vdots & \vdots \\ a_{xn} & 0 & a_{yn} & 0 & a_{zn} & 0 & -1 & 0 \end{bmatrix} \tag{12}$$

where $a_{xi} = \frac{\tilde{x}_i - \hat{x}_u}{\hat{r}_i}$, $a_{yi} = \frac{\tilde{y}_i - \hat{y}_u}{\hat{r}_i}$ and $a_{zi} = \frac{\tilde{z}_i - \hat{z}_u}{\hat{r}_i}$ with

$$\hat{r}_i = \sqrt{(\tilde{x}_i - \hat{x}_u)^2 + (\tilde{y}_i - \hat{y}_u)^2 + (\tilde{z}_i - \hat{z}_u)^2} \tag{13}$$

and

$$[\hat{x}_u \, \hat{y}_u \, \hat{z}_u]^T = [\hat{x}_u(k \mid k-1) \, \hat{y}_u(k \mid k-1) \, \hat{z}_u(k \mid k-1)]^T \tag{14}$$

4. Integrity

The positioning estimates obtained with a GNSS system are not absolutely accurate. Besides the errors discussed in section 2.1 some other malfunctions can lead to bigger errors that could compromise the navigation solution.

In civil aviation strict requirements are imposed on levels of precision, integrity, continuity and availability of the service. Integrity is the measure of the trust that can be placed in the correctness of the information supplied by a navigation system and includes the ability of the system to provide timely warnings to the user when the service should not be used [13]. Integrity is defined by the integrity risk, time to alert and alert limit requirements [15]:

- **Integrity Risk**: Is the probability of an undetected failure of specified accuracy. It is expressed per hour or per operation.

  A position failure is defined to occur whenever the position solution error exceeds the applicable xPL or xAL (if the equipment is aware of the navigation mode). xPL stands for Horizontal or Vertical Protection Level and xAL stands for Horizontal or Vertical Alert Limit.

- **Time to Alert**: It is the maximum allowable time interval between system performance ceasing to meet operational performance limits and the appropriate integrity monitoring subsystem providing an alert.

- **Alert Limits**: For each phase of flight, to ensure that position error is acceptable, alert limits are defined that represent the largest position error which result in a safe operation.

Integrity is one of the most essential aspects in navigation as abnormal positioning results would reflect in safety. Integrity anomalies are a rare occurrence, accounting only for a couple of times a year, but can be critical especially in aviation. The three main sources of errors that could lead to integrity problems are: satellite clocks, ephemeris errors and faults of main control station [10].

Ground Segment of GNSS systems controls the health status of the satellites to ensure that messages do not degrade beyond specified operational tolerances. However not all satellites are visible all the time by control stations so an anomaly in one of the satellites could take up to a few hours to be identified and disseminated by the control segment [8]. To overcome these limitations there are several integrity architectures to provide integrity to critical applications like aviation. Three different architectures have been proposed to provide integrity to the aviation community [4]:

- SBAS - Satellite-Based Augmentation System
- GBAS - Ground base augmentation System
- ABAS- Aircraft-Based Augmentation System
  - RAIM - Receiver Autonomous Integrity Monitoring
  - AAIM - Airborne Autonomous Integrity Monitoring

4.1. RAIM

RAIM is a user algorithm that determines the integrity of the GNSS solution. When more satellites are available than needed to have a position fix (satellite number > 4), the extra pseudoranges should be consistent with the computed position.

If the pseudorange from one satellite differs significantly from the expected value some fault may be associated with it or with another signal integrity problem. A key assumption usually made in RAIM algorithms for civil aviation is that only one satellite may be faulty, mainly because the probability of multiple satellite failures is negligible [8].

In order for a receiver to use a RAIM algorithm it is necessary to have a minimum of five visible satellites with a good geometry. With five satellites available we can use an algorithm called Fault Detection (FD). If six or more satellites are available we can use a more sophisticated algorithm called Fault Detection and Exclusion (FDE).

4.1.1 FD

Fault detection algorithm can be used with only five satellites visible. With five satellites available we can make five subsets of four satellites. The position solutions obtained by the various subsets are analysed for consistency, and an alert is provided if that consistency check fails. With this technique the receiver only detects an anomaly but the satellite in question is not identified.

Exemplifying, let's suppose 5 satellites are available: Satellites $(1, 2, 3, 4, 5)$. Let's assume that satellite 1 is faulty. With these 5 satellites, 5 subsets of 4 are possible:

Subset index	Subset	Solution
1	1,2,3,4	Faulty
2	1,2,3,5	Faulty
3	1,2,4,5	Faulty
4	1,3,4,5	Faulty
5	2,3,4,5	Correct

Table 1: Subsets of the available 5 satellites

If satellite 1 is faulty only the last subset would allow to compute the correct user position but RAIM algorithms cannot be used in these subsets, as at least 5 satellites are needed because with 4 satellites there would be no redundancy, so no exclusion can be performed. The navigation solutions obtained with 5 subsets are not consistent among themselves: they lead to different results. However, the RAIM algorithm is not able to decide which is the right solution.

4.1.2 FDE

A more sophisticated algorithm is FDE. To use this algorithm a minimum of six visible satellites are needed, not only to detect a fault but also exclude the faulty satellite from the solution. In fact the big difference from the FD algorithm is that, as the faulty satellite is excluded, navigation can continue without interruption.

Exemplifying, let's suppose 6 satellites are available: Satellites $(1, 2, 3, 4, 5, 6)$. Let's assume that satellite 1 is faulty. With these 6 satellites 6 subsets of 5 are possible:

Subset index	Subset	Solution
1	1,2,3,4,5	Faulty
2	1,2,3,4,6	Faulty
3	1,2,3,5,6	Faulty
4	1,2,4,5,6	Faulty
5	1,3,4,5,6	Faulty
6	2,3,4,5,6	Correct

Table 2: Subsets of the available 6 satellites

If satellite 1 is faulty, again, only the last solution would allow to compute the right position in a consistent way. To get to this conclusion the algorithm should analyse the $(n-1)$ subsets and search for subsets without fault detection condition, using the test statistics for the subsets. Since the faulty satellite is included in all subsets but one, only one subset, $(2, 3, 4, 5, 6)$, is free from the error of the faulty satellite and leads to 5 consistent navigation solutions. Concluding this, the satellite missing from the subset that does not have the fault condition is identified as the faulty satellite and exclusion can be performed [6].

4.1.3 RAIM algorithms

There are a variety of RAIM algorithms but all those algorithms include the following functions:

1. Have an observable discriminator called test statistic, which shows the effect of a faulty measurement with a bias error;
2. Know the likely noise in the system and their interactions with the test statistic, so that the relationship between the test statistic and the faulty measurement can be statistically described;
3. Establish a fault-free limit for the test statistic which will only, rarely, be exceeded by the observed test statistic when there is no faulty measurement. This fault-free limit, called the detection threshold, is typically based on a specific false alarm probability for the particular RAIM application;
4. Perform the detection test by comparing the observed test statistic against the detection threshold, meaning:
    - if the test statistic is less than the limit, then declare that no fault is present;
    - if the test statistic is equal to or greater than the limit, then declare that a fault has been detected and issue an integrity alarm.

5. In case of a fault, depending on the satellites available, two techniques can be applied:
   - If only 4 satellites are available integrity cannot be provided as at least 5 satellites are needed;
   - If 5 satellites are available fault detection can be performed;
   - If 6 or more satellites are available fault detection and exclusion can be performed.
6. Compute the protection levels (This step is optional and not taken into account in this thesis).

The two methods that are being analysed and performance tested in this thesis are the Least-Square Residuals and the Range Comparison Method. The analysis is partially based on [9].

Least-Squares-Residuals (LSR) Considering noisy pseudoranges from n satellites to be given by

$$y = \begin{bmatrix} U_1 \\ \vdots \\ U_n \end{bmatrix} + \begin{bmatrix} \epsilon_1 \\ \vdots \\ \epsilon_n \end{bmatrix} \tag{15}$$

and the pseudorange from the satellite i is given by

$$U_i = \sqrt{(X_i - x_u)^2 + (Y_i - y_u)^2 + (Z_i - z_u)^2} + c\Delta T \tag{16}$$

Considering (15) and (16) the corresponding incremental equations is

$$\Delta y = G\Delta x + \epsilon \tag{17}$$

with $\epsilon = [\epsilon_1 \dots \epsilon_n]$.

The incremental solution corresponding to (17) is

$$\Delta x = (G^T G)^{-1} G^T \Delta y \tag{18}$$

Thus, the least squares solution is

$$\hat{x}_{ls} = \hat{x}_{pred} + (G^T G)^{-1} G^T (y - \hat{y}_{pred}) \tag{19}$$

where $\hat{x}_{pred}$ and $\hat{y}_{pred}$ are respectively the predicted position and corresponding pseudorange vector, and G is the linearised measurement connection matrix which consists of the line-of-sight (LOS) vectors to the satellites, with *ones* in the fourth column corresponding to the clock bias [2].

The pseudorange vector may be reconstructed from (19) as

$$\begin{aligned} \hat{y} &= \hat{y}_{pred} + G(\hat{x}_{ls} - \hat{x}_{pred}) \\ &= \hat{y}_{pred} + G(G^T G)^{-1} G^T (y - \hat{y}_{pred}) \end{aligned} \tag{20}$$

and the residuals $w \equiv y - \hat{y}$ result from

$$\begin{aligned} w &= y - \hat{y}_{pred} - G(G^T G)^{-1} G^T (y - \hat{y}_{pred}) \\ &= [I - G(G^T G)^{-1} G^T](y - \hat{y}_{pred}) \end{aligned} \tag{21}$$

We can obtain the sum of the squared errors from the residuals by

$$SSE = w^T w = \epsilon^T S^2 \epsilon = \epsilon^T S \epsilon \tag{22}$$

Consider the test statistic

$$t = \sqrt{\frac{SSE}{n-4}} \tag{23}$$

Fault detection is based on the hypothesis testing where the decision variable t is tested against an alert threshold λ. The decision criteria is

$$\begin{cases} t \geq \lambda \rightarrow fault \\ t < \lambda \rightarrow no \quad fault \end{cases} \tag{24}$$

Range-Comparison Method (RCM) Another method to provide integrity considered in this thesis is the Range comparison method. With two methods one can validate the results and compare their performance.

Consider we use n satellites measurements

$$y = \begin{bmatrix} \tilde{y} \\ \cdots \\ \breve{y} \end{bmatrix} \tag{25}$$

where

$$\tilde{y} = \begin{bmatrix} y_1 \\ \vdots \\ y_4 \end{bmatrix}, \quad \breve{y} = \begin{bmatrix} y_5 \\ \vdots \\ y_n \end{bmatrix} \tag{26}$$

In this method the position is solved for the first four measurements $\tilde{y}$ where the order of the n equations is immaterial [2]. The resulting solution is then used to predict the remaining $n-4$ measurements and the predicted values are compared with the actual measured $\breve{y}$. If the $n-4$ residuals are small, we will have near-consistency in the measurements and the algorithm will declare *no failure*. On the contrary if one or several residuals are large, it will declare *failure* [2].

Let matrix G be partitioned as

$$G = \begin{bmatrix} \tilde{G} \\ \cdots \\ \breve{G} \end{bmatrix} \tag{27}$$

with $\tilde{G}(4 \times 4)$ and $\breve{G}((n-4) \times 4)$. Then according to (21)

$$\begin{bmatrix} \hat{y_1} \\ \vdots \\ \hat{y_4} \end{bmatrix} = \begin{bmatrix} \hat{y}_{1,pred} \\ \vdots \\ \hat{y}_{4,pred} \end{bmatrix} + \tilde{G}(\hat{x}_{ls} - \hat{x}_{pred}) \tag{28}$$

and

$$\begin{bmatrix} \hat{y}_5 \\ \vdots \\ \hat{y}_n \end{bmatrix} = \begin{bmatrix} \hat{y}_{5,pred} \\ \vdots \\ \hat{y}_{n,pred} \end{bmatrix} + \breve{G}(\hat{x}_{ls} - \hat{x}_{pred}) \tag{29}$$

As

$$\hat{x}_{ls} = \hat{x}_{pred} + \tilde{G}^{-1}\left(\begin{bmatrix} y_1 \\ \vdots \\ y_4 \end{bmatrix} - \begin{bmatrix} \hat{y}_{1,pred} \\ \vdots \\ \hat{y}_{4,pred} \end{bmatrix}\right) \quad (30)$$

then

$$\begin{bmatrix} \hat{y}_5 \\ \vdots \\ \hat{y}_n \end{bmatrix} = \begin{bmatrix} \hat{y}_{5,pred} \\ \vdots \\ \hat{y}_{n,pred} \end{bmatrix} + H\left(\begin{bmatrix} y_1 \\ \vdots \\ y_4 \end{bmatrix} - \begin{bmatrix} \hat{y}_{1,pred} \\ \vdots \\ \hat{y}_{4,pred} \end{bmatrix}\right) \quad (31)$$

where $H((n-4)\times 4)$ is defined as

$$H = \breve{G}\tilde{G}^{-1} \quad (32)$$

Solution for $n = 5$ satellites Let us now consider the case when 5 satellites are used in the RCM method. In this case matrix $\tilde{G}$ is (4×4) and $\breve{G}$ is (1×4). Given (32), matrix H is defined by

$$H = \begin{bmatrix} h_{11} & h_{12} & h_{13} & h_{14} \end{bmatrix} \quad (33)$$

In this case, the residuals vector w is reduced to a scalar w_1 we have

$$\sigma_1^2 = E\{w_1^2\} = \sigma^2(HH^T + 1) = \sigma^2\left(1 + \sum_{i=1}^{4} h_{1i}^2\right) \quad (34)$$

The probability density function of w_1 in the absence of any satellite malfunction is

$$p_w(w_1) = \frac{1}{\sqrt{2\pi\sigma_1^2}}\exp\left(-\frac{w_1^2}{2\sigma_1^2}\right) \quad (35)$$

Let us now consider the decision rule that divides the real axis in three distinct regions, $|w_1| < \lambda_1$, corresponding to the hypothesis of *no-failure*, and $|w_1| \geq \lambda_1$, corresponding to the hypothesis of satellite *failure*. This decision rule is illustrated in figure 1.

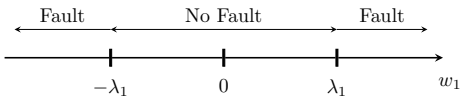

Figure 1: Decision rule for the Range-Comparison Method when 5 satellites are used

The probability of false alarm is

$$P_{fa} = 1 - \int_{-\lambda_1}^{\lambda_1} p_w(w_1)dw_1 = 2Q\left(\frac{\lambda_1}{\sigma_1}\right) \quad (36)$$

Solution for $n = 6$ satellites Let us now consider the case when 6 satellites are used in the RCM method. In this case matrix $\tilde{G}$ is (4×4) and $\breve{G}$ is (2×4). Given (32), matrix H is defined by

$$H = \begin{bmatrix} h_{11} & h_{12} & h_{13} & h_{14} \\ h_{21} & h_{22} & h_{23} & h_{24} \end{bmatrix} \quad (37)$$

In this case the Gaussian vector of residuals is given by $w = \begin{bmatrix} w_1 & w_2 \end{bmatrix}$. In a no-fault scenario the covariance matrix is

$$E\{ww^T\} = \sigma^2[HH^T + I] = \begin{bmatrix} \sigma_1^2 & \rho\sigma_1\sigma_2 \\ \rho\sigma_1\sigma_2 & \sigma_2^2 \end{bmatrix} \quad (38)$$

where

$$\sigma_1^2 = \sigma^2\left(1 + \sum_{i=1}^{4} h_{1i}^2\right) \quad (39)$$

$$\sigma_2^2 = \sigma^2\left(1 + \sum_{i=1}^{4} h_{2i}^2\right) \quad (40)$$

and the correlation coefficient is

$$\rho = \frac{\sum_{i=1}^{4} h_{1i}h_{2i}}{\sqrt{1+\sum_{i=1}^{4} h_{1i}^2}\sqrt{1+\sum_{i=1}^{4} h_{1i}^2}} \quad (41)$$

The integral of the joint probability density function of $p_w(w_1, w_2)$ over an area A, is bounded by the ellipse

$$\left(\frac{w_1}{\sigma 1}\right)^2 - \frac{2\rho w_1 w_2}{\sigma_1\sigma_2} + \left(\frac{w_2}{\sigma_2}\right)^2 = \alpha^2(1-\rho^2) \quad (42)$$

is given by [7]

$$\int\int_A p_w(w_1, w_2)dw_1dw_2 = 1 - \exp\left(-\frac{\alpha^2}{2}\right) \quad (43)$$

Let us now consider a decision rule that divides the plane into two distinct regions, one hypothesis corresponding to *no failure* and other the to *failure*. A common way to choose the decision boundary is to let it be an equal probability density contour, conditioned to the assumption of no satellite malfunction, according to (42) [2].

The probability of false alarm is

$$p_{fa} = 1 - \int\int_A p_w(w_1w_2)dw_1dw_2 = \exp\left(-\frac{\alpha^2}{2}\right) \quad (44)$$

such that the *failure/no failure* decision boundary is given by (42), that is

$$\left(\frac{w_1}{\sigma_1}\right) - \frac{2\rho w_1 w_2}{\sigma_1\sigma_2} + \left(\frac{w_2}{\sigma_2}\right)^2 = -2(1-\rho^2)ln(P_{fa}) \quad (45)$$

4.2. Integrity in Galileo

The integrity concept introduced by Galileo consists in providing the users with data enabling them to monitor their integrity level.

Galileo has the capability to monitor the satellite behaviour through its complex global distributed ground network consisting of more than 30 sensor stations. Taking these measurements into account, satellite failures (due to orbit or clock inaccuracies)

can be detected and alerts can be disseminated to the user.

The SoL service is particularly studied since it is the one to provide users with integrity information. The nature of the provided information consists in three parameters per satellite:

- Signal-In-Space Accuracy (SISA)
- Signal-In-Space Monitoring Accuracy (SISMA)
- Integrity Flag (IF)

These three parameters relate to Signal-In-Space Error (SISE) [11] [3].

A particular algorithm has been introduced in [12] to make best use from the integrity data provided in the Safety-of-Life service. The analysis of this topic follows essentially [15].

The final expression of the global (i.e taking into account vertical and horizontal errors, in both fault-free and faulty cases) integrity risk P_{IR} at the alert limits HAL and VAL is [15]:

$$\begin{aligned} &P_{IR}(HAL,VAL) = P_{IR,V} + P_{IR,H} \\ &= 1 - \text{erf}\left(\frac{VAL}{\sqrt{2}\sigma_{V,FF}}\right) + \exp^{-\frac{\text{HAL}^2}{\xi_{FF}^2}} \\ &+ \frac{1}{2}\sum_{j=1}^{N} P_{SatFail,j}\left(\left(1 - \text{erf}\left(\frac{VAL + \mu_{V,j}}{\sqrt{2}\sigma_{V,j,FM}}\right)\right) + \left(1 - \text{erf}\left(\frac{VAL - \mu_{V,j}}{\sqrt{2}\sigma_{V,j,FM}}\right)\right)\right) \\ &+ \sum_{j=1}^{N} P_{SatFail,j}\left(1 - S_{\chi_2^2,\delta_j}\left(\frac{HAL^2}{\xi_{FM}^2}\right)\right) \end{aligned} \tag{46}$$

5. Computer Simulation Procedure

To perform the computer simulations a GPS constellation was simulated with parameters used from YUMA almanac file format. After the definition of the GPS constellation and after the user position is defined, the satellites with an elevation angle above 10° are considered visible.

To be able to perform detection and exclusion a set of 6 satellites is chosen with the lowest GDOP value, to achieve lower error in position results. After the selection of the 6 satellites a trajectory is simulated and the user position is calculated, the test statistic t is calculated and compared to the threshold λ. The results from this comparison can be grouped according:

- No faulty satellites
    1. If $t < \lambda$ we have a normal operation with probability of $1 - P_{fa}$
    2. If $t \geq \lambda$ we have a false alarm with probability P_{fa}.
- Presence of a faulty satellite
    1. If $t \geq \lambda$ we have an integrity alarm with probability $1 - P_{md}$;
    2. If $t < \lambda$ we have a missed detection with probability of P_{md}.

5.1. Computer Simulation Results

5.1.1 RAIM Algorithms Performance Analysis

To measure and compare the performance of the RAIM algorithms discussed in section 4.1.3 a series of Monte Carlo simulations are performed.

To investigate the probability of error detection, two types of error can be induced to the measurements [6]:

- A slow ramp;
- A step error.

To test both algorithms, two epochs were used. The first epoch was on 22/01/2015 at 16:40 and the second on 22/01/2015 at 19:20. The purpose of using two epochs is to test two distinct geometries to see how the two algorithms perform under different test scenarios.

Performance analysis with no error To test the false alert requirement the algorithms should run without any positioning failure induced, since the false alarm probability assumes that no real positioning failure is present.

The results from this test for both methods showed that the experimental P_{fa} was very similar to the theoretical value. The small discrepancy found can be due to the finite number of runs which can influence the final result.

Performance analysis with error induced To test the detection capability of the algorithms an error is induced to the measurements as referred in section 5.1.1.

The first test to be performed is the detection test with several values of step errors. To perform this test two epochs are analysed and each satellite in the subset will have a step error induced to their measurements at a time.

In cases of poor satellite geometry DOP values get large and the navigation accuracy degrades. A similar effect occurs with RAIM algorithms [1]. When the satellite geometry is poor the performance of the integrity monitoring algorithms degrade and large navigation errors can occur before they are detected, so it is important to understand how the detection capabilities of the algorithms varies depending on the satellite affected by the error.

Various criteria have been used for evaluating the quality of the satellite geometry for detection purposes [2]. The method used in this thesis is the $SLOPE_{max}$ method. The first simulation test was performed on 22/01/2015 at 16:40. At this time satellites 5, 13, 15, 21, 24, 28, 30 were visible and the subset of 6 satellites with lowest GDOP value was 5, 13, 15, 21, 24, 30 with a correspondent

GDOP of 2.3793. Let us now analyse the results with LSR method for this test. These results are shown in figure 2.

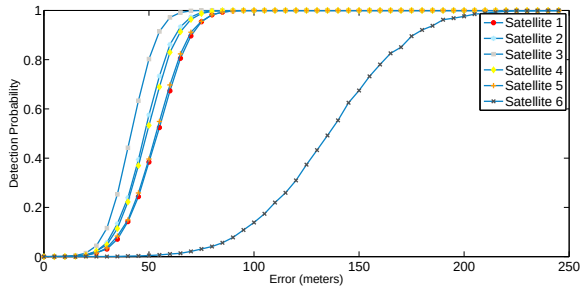

Figure 2: Detection probability versus error for LSR method

From the analysis of figure 2 we conclude that satellite 6 (corresponding to satellite ID 30) is the least sensitive to errors. This is easily noticeable because for the same amount of error induced in the various satellites of the subset, satellite 6 is the one that requires a larger error to reach 100% probability of detection.

Lets now analyse the results with Range Comparison Method for this same test. These results are shown in figure 3.

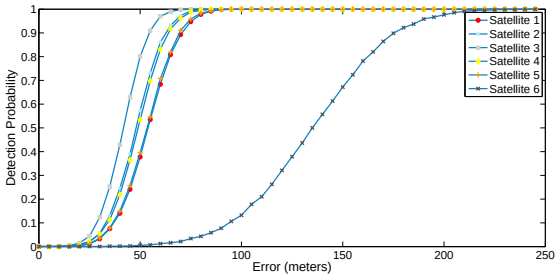

Figure 3: Detection probability versus error for RCM method

From the analysis of figure 3 we can see that the results are very similar for all the satellites. This lead us to conclude that the two methods are equally sensitive to induced errors in the measurements and that the methods are also equally sensitive to satellite geometry.

In figure 4 the probability of detection difference between the two methods is shown.

It's easily understandable that the differences are marginal and that the two methods have a very similar performance in the detection test. Also, these small differences that are verified may be associated with the limited number of runs that each test used.

After introducing these errors to test the algorithms for detection capabilities, a test of exclusion of the faulty satellites was performed for the first

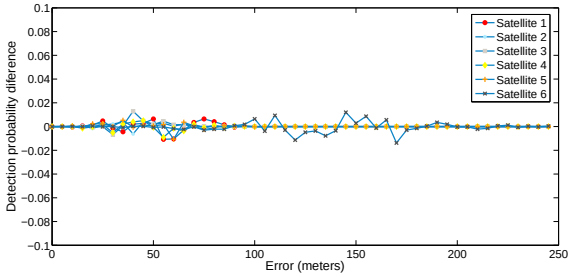

Figure 4: Detection probability difference between RCM and LSR method for the first epoch

test case. The method behind the exclusion of the faulty satellite was previously discussed in section 4.1.2. The results from this test are shown in figure 5.

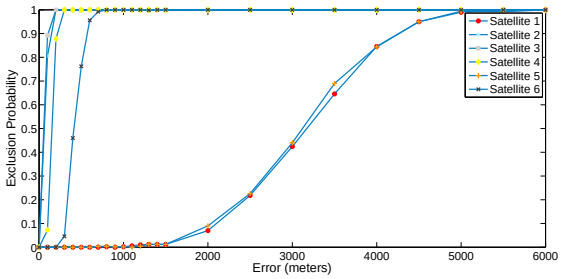

Figure 5: First exclusion simulation for LSR method

From the analysis of figure 5 we understand that the values of error that lead us to an exclusion level of 100% are substantially higher than the ones needed for detection only. This is due to the fact that for a satellite to get successfully excluded, that satellite has to be declared as faulty in all subsets, as explained in section 4.1.2. Actually, some subsets may have such geometries that large errors are needed for a detection to happen and that leads to large errors for the exclusion process.

For the test carried out on 22/01/2015 at 19:20, where conditions are slightly similar among the satellites, detection tests are performed for both methods.

The results from detection test for the LSR method are shown in figure 6.

From figure 6 we can confirm that in this case all satellites require similar values of error for the same detection probability to be obtained.

This same test was repeated for range comparison method and the results from this detection test are shown in figure 7.

As expected from previous comparatives between these two methods the results are very similar, and some of the residual differences may be due to the limited number of runs. This result increases our

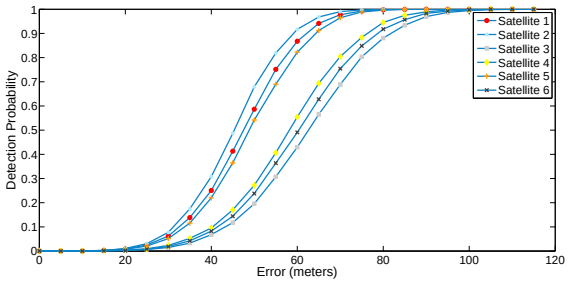

Figure 6: Second detection simulation for LSR method

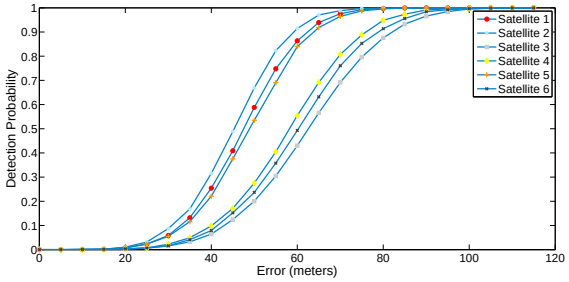

Figure 7: Second detection simulation for RCM method

confidence in saying that the two methods show the same sensitiveness to errors and satellite geometry as for epoch 1 the results were also very similar between the two methods.

Let us now analyse the results from an induced ramp error to the measurements. These tests will be relative to first epoch.

Two tests will be performed: one with a ramp with a slope of $1m/s$ and another with a slope of $0.1m/s$.

Starting with the higher slope ramp the results in terms of time of first detection are shown in table 3.

	Mean first time detection	Standard deviation
Satellite 1	36.29	7.38
Satellite 2	34.34	6.58
Satellite 3	30.31	6.12
Satellite 4	34.92	5.6
Satellite 5	36.96	7.03
Satellite 6	80.53	15.79

Table 3: Mean first detection time for LSR method (ramp 1 m/s)

From table 3 we can understand that for the first 5 satellites the first detections occur, in mean, a few moments after 30 seconds. As the slope of the error is 1m/s this corresponds to a mean value of error of about 30 meters. These values are according to the expected, as in figure 2 the first magnitude of errors that are being detected are errors of about 30 meters for the first 5 satellites. For the last satellite the mean value of first detection comes much later in time as for this satellite in this specific geometry a much larger error is needed for it to be detected. The standard deviation values around the first detection gives us one idea of how much centered about the first detection time the detection is.

In figure 8 an illustration of the test statistic variation with this ramp error is shown.

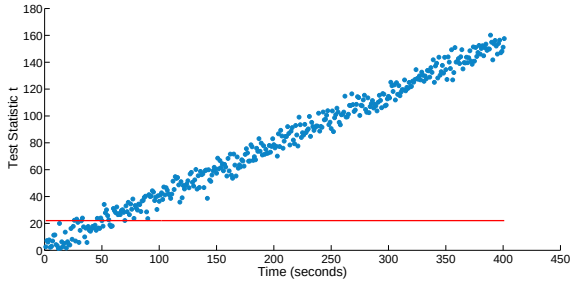

Figure 8: Test statistic variation over a ramp error of 1 m/s

The same test was performed for Range Comparison Method and the results are presented in table 4.

	Mean first time detection	Standard deviation
Satellite 1	37.16	6.32
Satellite 2	34.2	5.83
Satellite 3	29.16	5.58
Satellite 4	35.2	6.7
Satellite 5	39.14	6.98
Satellite 6	79.73	14.27

Table 4: Mean first detection time for RCM method (ramp 1 m/s)

From the analysis of table 4 we can conclude that, as expected from the results from previous tests, results are identical to those obtained with the LSR method. Slightly variations on the values reflect the limited number of simulations performed.

For the ramp bias with a slope of 0.1 m/s the two methods were also tested. The results for LSR are shown in table 5.

The results from table 5 show an obvious higher time to first detection as the slope is now 0.1 m/s. While with a slope of 1 m/s the magnitude of error for first detection was about 30 meters, for this slope we have a lower value of about 23 meters ($\sim 230s \times 0.1m/s$). This can be explained because as the slope is lower more points of the test statistic will be near the threshold, so is more probable that any point near it, due to random noise, can

	Mean first time detection	Standard deviation
Satellite 1	260.5	60.22
Satellite 2	223.6	48.79
Satellite 3	201.4	44
Satellite 4	239.5	55
Satellite 5	243	54
Satellite 6	513.4	139.4

Table 5: Mean first detection time for LSR method (ramp 0.1 m/s)

break the threshold counting for a earlier detection when compared to the higher slope. This fact is illustrated in figure 9.

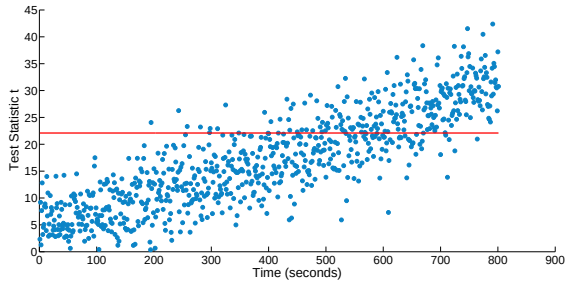

Figure 9: Test statistic variation over a ramp error of 0.1 m/s

This same test was also performed for the Range Comparison Method. For this method the results are shown in table 6.

	Mean first time detection	Standard deviation
Satellite 1	258.1	64.87
Satellite 2	226.3	53.84
Satellite 3	201.5	40.67
Satellite 4	234	57.3
Satellite 5	241	57.3
Satellite 6	502.9	125.7

Table 6: Mean first detection time for RCM method (ramp 0.1 m/s)

The values of table 6 show us very similar results comparing to the equivalent test performed with LSR which validates, once again, that the two methods have very similar performances even for slope errors.

6. Conclusions

The objectives of this thesis were to study and make a comparison of two algorithms implemented to provide receiver autonomous integrity. To make this study a GPS constellation was simulated from YUMA almanac parameters. The position solution from that trajectory was obtained using a Kalman filter. To test the performance of the algorithms a subset of 6 satellites with the best GDOP parameter was chosen among the visible satellites at the time of simulation. Two epochs were considered to test different geometries and to study how those differences could affect the algorithms performance.

Two two algorithms studied have different approaches to achieve the solution. The Least-Square-Residuals uses the estimated position solution from all satellites in the subset to predict the six measurements. The sum of squares of residuals is calculated and used as test statistic. In the range comparison method with 6 satellites in the subset the first 4 are used to obtain a solution and then that solution is used to predict the remaining 2 measurements.

Regardless of the different approaches of the two methods studied, the results from the simulation showed that the performance of both methods are almost identical in the various tests for the different geometries studied. The small differences verified are negligible and besides they can be also affected by the limited number of runs performed in each test.

The Least-Squares-Residuals RAIM method is specially simple in its implementation because the test statistic is a scalar regardless of the number of satellites in use. For the Range-Comparison-Method such is not the case and the implementation complexity raises as we use more satellites in the subset as the decision rule divides the plane in more regions to test the failure hypotheses.

As the Range-Comparison-Method showed no advantages in the tested cases, the Least-Squares-Residuals method is recommended because its performance is identical and the implementation is considerably less complex.

References

[1] A. Brown and M. Sturza. *The Effect of Geometry on Integrity Monitoring Performance.* Proceedings of the 46th Annual Meeting of The Institute of Navigation, 1990.

[2] R. Grover Brown. *A Baseline GPS RAIM Scheme and a Note on the Equivalence of Three RAIM Methods*, volume 39. NAVIGATION: Journal of The Institute of Navigation, Fall 1992.

[3] A. Mozo García, C. Hernández Medel, and M. Romay-Merino. *Galileo navigation and integrity algorithms.* Proceedings of the ION GNSS 18th International Meeting, 2005.

[4] ICAO, editor. *Standard and Recommended Procedures.* International Civil Aviation Organization.

[5] Elliott D. Kaplan and Christopher J. Hegarty. *Understanding GPS.* Artech House, second edition, 2006.

[6] Y. Lee, K. Van Dyke, B. Decleene, J. Studenny,

, and M. Bekmann. *Summary of RTCA SC-159 GPS Integrity Working Group Activities*. Navigation: Journal of The Institute of Navigation, 1996.

[7] I. Stegun M. Abramowitz. *Handbook of Mathematical Functions*. Dover Publications, 1970.

[8] Navipedia. Integrity. `http://www.navipedia.net/index.php/Integrity`, 2015. [accessed 01-February-2015].

[9] F. D. Nunes. *Notes on RAIM*. Internal Report IT/IST, June 2011.

[10] F. D. Nunes. *Sistemas de Controlo de Trafego*. 2013.

[11] V. Oehler, F. Luongo, J.-P. Boyero, R. Stalford, H. L. Trautenberg, J. Hahn, F. Amarillo, M. Crisci, B. Schlarmann, , and J.F. Flamand. *The GALILEO integrity concept*. Proceedings of the ION GNSS 17th International Meeting, September 2004.

[12] V. Oehler, H. L. Trautenberg, F. Luongo, J.-P. Boyero, , and B. Lobert. *User integrity risk calculation at the alert limit without fixed allocations*. Proceedings of the ION GNSS 17th International Meeting, September 2004.

[13] Department of Defense, editor. *Federeal Radionavigation Plan*. Department of Defense, Department of Homeland Security, and Department of Transportation of USA, 2008.

[14] P. Enge P. Misra. *Global Positioning System, Signals, Measurements, and Performance*. Ganga-Jamuna Press, 2001.

[15] M. Paimblanc. *Integrity risk in satellite radionavigation systems*. PhD thesis, L' Institut National Polytechnique de Toulouse, 2007.

[16] Patrick Y. C. Hwang R. G. Brown. *Introdution to Random Signals and Applied Kalman Filtering*. Wiley, third edition, 1997.